ISSN Online: 2821-1693

Transactions on Machine Intelligence

Journal Homepage: https://tmachineintelligence.ir/index.php/TMI

# Design and Development of a Knee Rehabilitation Robot to Improve Range of Motion and Strength in Injured Athletes

S. Javanshiri Vaziri[1,*], N. Mohammad Hashemi[2], K. Ghaemi Osgouie[3]

[1] MSc, Mechatronics Engineering, University of Tehran, International Campus – Kish Island, Iran
[2] PhD Candidate, Mechanical Engineering, Faculty of Engineering, University of Tehran, Tehran, Iran
[3] Assistant Professor, Mechanical Engineering, Faculty of Engineering, University of Tehran, Tehran, Iran

**ARTICLE INFO**

Article History:
Received 26 December 2024
Received in revised form 15 January 2025
Accepted 9 February 2025
Available online 14 March 2025

Keywords:
Genetic Algorithm, Rehabilitation, Kinematics, Robot, Knee Joint.

**ABSTRACT**

The knee joint, being the largest and most complex synovial joint in the body, plays a crucial role in weight-bearing and bodily movements. Due to its wide range of motion, the knee joint is highly vulnerable to injury, and damage to it can lead to movement limitations, significant disability, and a reduction in the quality of life. The use of robotics in rehabilitation has attracted significant attention in knee rehabilitation exercises, offering extensive capabilities for functional adaptation of knee movements in injured athletes. This study focuses on the knee joint's musculoskeletal structure and dynamics, using mathematical modeling and simulation to analyze its behavior. The goal of this research is to identify the forces, torques, and reaction forces in the tibiofemoral joint (the connection between the shinbone and femur) to design and develop a rehabilitation device that reduces knee injuries and is suitable for athletes of different weights and heights. In designing this sports device, emphasis is placed on reducing the negative effects of variable forces on the knee muscles, particularly at angles where the forces reach their maximum. The ultimate goal is to reduce the risk of injury in this area. Furthermore, the device should be designed to be adjustable for athletes of different body sizes, which can be achieved by applying standard settings based on the actual forces exerted on the knee. Lastly, a genetic algorithm is used to optimize the lengths of the links and their placement in the mechanism.

## 1. INTRODUCTION

The knee joint is one of the most essential and complex joints in the human body. Due to its wide range of motion, it is particularly vulnerable to injury. Knee injuries are especially common among athletes because of the demanding and complex movements they perform. These injuries may include tears of the anterior cruciate ligament (ACL), posterior cruciate ligament (PCL), meniscus, and articular cartilage. Rehabilitation following knee injury is critical for returning to normal daily activities and athletic performance. Traditional rehabilitation methods—such as physiotherapy, strength training, and hydrotherapy—play a significant role in improving range of motion, muscle

* Corresponding Author: sarajavanshirivaziri@gmail.com
MSc, Mechatronics Engineering, University of Tehran, International Campus – Kish Island, Iran



http://dx.doi.org/10.47176/TMI.2025.26

strength, and joint stability. However, these methods can be time-consuming, physically demanding, and often require constant supervision by specialists.

In recent years, the integration of robotics into knee rehabilitation has emerged as a promising and effective approach. Robotic knee rehabilitation systems can apply precise, controlled movements to the joint while continuously monitoring the patient's progress through real-time feedback. These systems can deliver highly personalized rehabilitation programs tailored to each patient's condition, thus accelerating recovery and improving outcomes. One of the key advantages of robotic rehabilitation is the ability to simulate natural knee movements. These robots can accurately replicate complex motions such as flexion, extension, internal rotation, and external rotation. This allows patients to regain their natural range of motion and relearn proper movement patterns.

Furthermore, robotic systems can apply targeted, controlled resistance to the muscles surrounding the knee, aiding in the strengthening of weakened muscle groups. Muscle strength around the knee is essential for joint stability and injury prevention. In addition, robotic rehabilitation systems provide real-time feedback to patients regarding their motor performance, enabling them to correct improper movement patterns and enhance functional outcomes.

Several studies have explored the biomechanics of knee motion and its implications for rehabilitation. For instance, Sawhney et al. investigated the effect of isometric quadriceps contraction on femoral displacement in individuals with healthy knees. Their findings indicated that during open kinetic chain (OKC) exercises with 10 pounds of distal resistance, significant anterior displacement of the femur occurred at knee flexion angles of 30° and 45°, whereas femoral movement was significantly reduced at 60° and 75° of flexion. They also observed that the quadriceps neutral angle ranged between 60° and 75° of flexion. At flexion angles less than the neutral position, OKC stretching increased quadriceps activation, resulting in greater anterior femoral displacement. In contrast, at angles beyond the neutral position, OKC movements triggered higher hamstring activation, leading to posterior femoral displacement [1].

Beynnon et al. used a Hall-effect transducer to measure forces applied to the ACL during common knee rehabilitation exercises. Their results showed that OKC knee extension exercises generate strain on the ACL, depending on the knee flexion angle and the level of quadriceps activity [2]. Researchers have identified several conditions and activities that produce tensile stress on the healthy ACL. Studies suggest that active quadriceps contraction without external loading can create undesirable anterior shear forces on the tibia, particularly at flexion angles between 30° and full extension. These shear forces progressively increase with knee extension and may endanger the healing ACL graft. Consequently, some specialists recommend limiting quadriceps strengthening exercises to knee flexion angles between 30° and 90° to minimize shear stress on the ACL and reduce the risk of reinjury [3-4].

It is also important to note that patellofemoral pain syndrome is one of the most common complications following ACL reconstruction [3-6]. Some researchers argue that the recommended exercise angles may trigger or exacerbate patellofemoral symptoms [7]. Specifically, quadriceps exercises during the final 30° of extension are contraindicated in the early stages of ACL rehabilitation but are necessary for managing patellofemoral syndrome [3]. This creates a so-called "rehabilitation paradox": while movements beyond 30° of flexion help protect the patella, they simultaneously generate high forces that may compromise the healing ACL graft [3-5].

In this study, we aim to design and develop a knee rehabilitation robot to improve range of motion and muscular strength in injured athletes. The robot is engineered using a dynamic model of the knee joint and optimized control algorithms. It is capable of accurately simulating complex knee movements and applying precisely controlled resistance to the surrounding musculature. Additionally, the robot provides real-time feedback on the patient's motor performance.

To support the design process, we first conduct a biomechanical analysis of the knee joint's musculoskeletal structure through mathematical modeling to estimate forces, torques, moments, and reaction forces at the tibiofemoral joint. Necessary simulations are then performed to understand the joint's dynamic behavior. Finally, a genetic algorithm is employed to optimize the link lengths and positions in the robot's mechanism. These simulations are carried out using SolidWorks software.

## 2. MUSCULOSKELETAL STRUCTURE OF THE KNEE JOINT

The knee joint, as the largest and most complex synovial joint in the body, plays a vital role in various human movements. This joint is a combination of three distinct joints, including the joint between the femur and patella, as well as two joints between the femoral condyles and the tibia. The wide range of motion of the knee allows humans to perform a variety of activities, ranging from walking and running to bending and jumping. However, the distribution of weight across this joint in various positions makes the precise evaluation of weight distribution and force vectors a complex task. Since the knee joint bears most of the body's weight, it is highly vulnerable to impact and excessive forces. Knee injuries can lead to functional limitations and significant disability. Therefore, understanding the anatomy and biomechanics of this joint is crucial.

The lower part of the femur and the upper part of the tibia (shin bone) are connected through multiple ligaments within the knee joint. The patella is a small bone at the front of the knee joint. These three bones form the synovial (diarthrodial) knee joint, which is an example of a hinge joint with an elliptical shape that allows both rolling and sliding motions [8]. Figure 1 illustrates the movements of the knee joint and shows an example of a hinge joint similar to the tibiofemoral joint. The patella can slide along the groove of the femur because it is connected to the tibia at the bottom via the patellar tendon and to the quadriceps muscles at the top via the quadriceps tendon. The articular cartilage on the surfaces of the bones in the joint forms the primary interface. The ligaments stabilizing the tibiofemoral joint are shown in Figure 2.

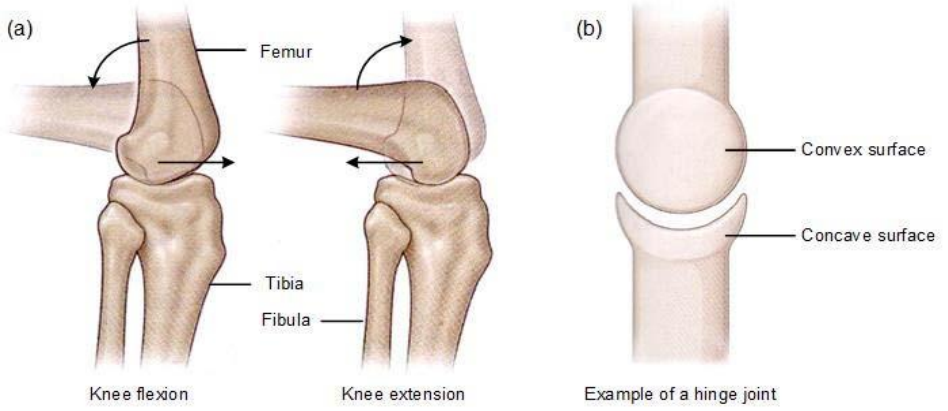


**Fig. 1.** (a) Lateral view of the tibiofemoral joint showing rolling and sliding during flexion and extension, and (b) the convex-concave surfaces of the hinge joint.

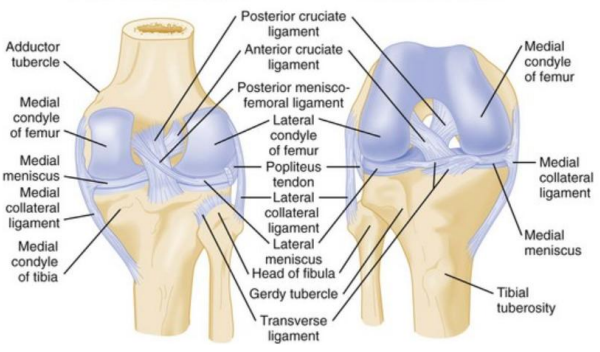


**Fig. 2.** Ligaments of the tibiofemoral joint: anterior view and posterior view of the right knee joint.

Ligaments are strong bands of connective tissue responsible for connecting bones to each other and maintaining joint stability. The knee joint, as the most complex joint in the human body, relies on four primary ligaments for its stability and proper function: the anterior cruciate ligament (ACL), posterior cruciate ligament (PCL), medial collateral ligament (MCL), and lateral collateral ligament (LCL). Along with muscles and tendons, these ligaments maintain knee joint stability during various movements such as bending, straightening, and rotation. By exerting tension and pressure against excessive joint movements, they prevent damage to cartilage and bones.

Most of the mechanical impact forces in the knee joint are generated and absorbed by the menisci. The total mass of the menisci is much greater than the articular cartilage, which bears the load across the entire knee joint. The deformability of the menisci, with their low compressive, shear, and permeability stiffness, ensures proper load distribution within the knee joint. The knee joint primarily allows one degree of freedom (DoF) for motion, which is described as flexion and extension, while also permitting slight internal and external rotation, classifying it as two degrees of freedom (2 DoF) joint. The muscle groups corresponding to the movements of the knee joint are shown in Table 1.

**Table 1.** Knee joint movements and muscle groups [8]

| Knee Movements | Muscle Groups | |
|---|---|---|
| 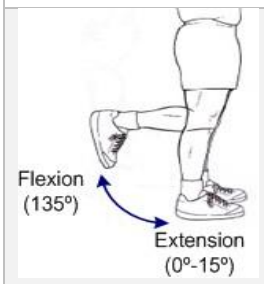 | **Extensor**<br>1. Rectus femoris<br>2. Vastus lateralis<br>3. Vastus intermedius<br>4. Vastus medialis | **Flexor**<br>1. Sartorius<br>2. Gracilis<br>3. Biceps femoris<br>4. Semimembranosus<br>5. Semitendinosus<br>6. Plantaris<br>7. Popliteus<br>8. Gastrocnemius |
| 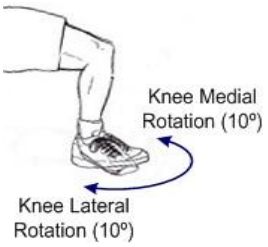 | **Lateral Rotator**<br>1. Biceps femoris | **Medial Rotator**<br>1. Gracilis<br>2. Sartorius<br>3. Semimembranosus<br>4. Semitendinosus<br>5. Popliteus |

## 3. KINEMATICS OF THE KNEE JOINT

To understand the mechanics of the knee joint, the sitting posture is considered, as shown in Figure 3, where the torso and thigh are in a resting position, while the distal part of the lower limb (the shin and foot) moves freely along the rotational axis of the knee joint. The parameters presented in equation (1) are used to calculate the quadriceps force (hip joint) ($F_{QF}$) [9-14]. Equation (2) represents the force required in the quadriceps muscles to maintain the knee at an angle $\theta_1$ [15].

$$\left.\begin{array}{r} Mass\ of\ Shank\ (\approx\ X_s\% = 4.7\%\ of\ BW) = m_{\text{snk}} \\ Mass\ of\ foot\ (\approx\ Y_f\% = 1.5\%\ of\ BW) = m_{foot} \\ Length\ of\ Shank\ (\approx\ B_s\% = 24.7\%\ of\ BH) = l_{\text{snk}} \\ Length\ of\ CoM\ of\ Shank\ (\approx\ A_s\% = 43.3\%\ of\ lsnk) = l_{coM_{snk}} \\ Height\ of\ Foot\ or\ Ankle\ (\approx\ B_f\% = 4.2\%\ of\ BH) = l_{foot} \\ Height\ of\ Foot\ CoM\ (\approx\ A_f\% = 50\%\ of\ foot) = l_{coM_{foot}} \\ Moment\ arm\ of\ Quadriceps\ Femoris\ (0.04m) = l_{QF} \\ Angle\ of\ Patelar\ Tendon\ (PT)(15°) = \theta_{\text{PT}} \end{array}\right\} \quad (1)$$

$$F_{QF} = \frac{\left(m_{\text{snk}}.g.l_{coM_{snk}}.\cos\theta_1\right) + \left(m_{\text{foot}}.g.\left(l_{\text{snk}} + l_{coM_{foot}}\right).\cos\theta_1\right)}{l_{QF}\sin\theta_{PT}} \quad (2)$$

The calculation of the internal torque ($M_{int}$) of the shin section is shown in equation (3) [15], and Figure 4 illustrates the internal torque of the shin section.

$$M_{int_{leg}} = \left(m_{snk}.l_{coM_{snk}}\right) + \left(m_{\text{foot}}.\left(l_{\text{snk}} + l_{coM_{foot}}\right)\right) \quad (3)$$

The components of the reaction force in the x and y directions ($J_F$), ( $J_{FX}$,$J_{FY}$) are shown in Figure 5. Equations (4) and (5) represent the reaction force at the knee joint while the foot is held at an angle of θ1 [15]. Using trigonometric relationships, the direction of the reaction force ($\theta_J$) can also be calculated, as shown in equation (6) [15].

$$J_{FX} = \left(F_{QF}.\cos\theta_{PT}\right) + \left(m_{\text{snk}}.g.\sin\theta_1\right) + \left(m_{\text{foot}}.g.\sin\theta_1\right) \quad (4)$$

$$J_{FY} = \left(F_{QF}.\sin\theta_{PT}\right) + \left(m_{\text{snk}}.g.\text{Cos}\,\theta_1\right) + \left(m_{\text{foot}}.g.\cos\theta_1\right) \quad (5)$$

$$\theta_J = \cos^{-1}\left(\frac{J_{FX}}{J_F}\right) \quad (6)$$

The necessary parameters for calculating the torque generated at the knee joint for a given angle are shown in Figure 6. Equations (7), (8), and (9) demonstrate how to calculate the mass and center of mass (COM) positions for the shin, foot, and entire lower limb based on reference data [9-12]. Here, $m_{\text{snk}}$ , $m_{\text{foot}}$ refer to the mass of the shin and the entire foot, respectively. Additionally, the lengths of the shin, the center of mass of the shin, and the center of mass of the foot are represented by ‘$l_{\text{snk}}$ $l_{coM_{snk}}$ and $l_{coM_{foot}}$, respectively.

$$\left.\begin{array}{l} m_{snk} = X_s\%\ of\ BW = \left(\frac{X_s}{100}\right).BW \\ m_{\text{foot}} = Y_f\%\ of\ BW = \left(\frac{Y_f}{100}\right).BW \end{array}\right\} \quad (7)$$

$$\left.\begin{array}{l} l_{\text{snk}} = B_s\%\ of\ BH = \left(\frac{B_s}{100}\right).BH \\ l_{coM_{snk}} = A_s\%\ of\ B_s\%\ of\ BH = \left(\frac{A_s.B_s}{1000}\right).BH \\ l_{coM_{foot}} = A_s\%\ of\ B_s\%\ of\ BH = \left(\frac{A_s.B_s}{1000}\right).BH \end{array}\right\} \quad (8)$$

$$m_{leg} = \left(m_{snk} + m_{foot}\right)$$

$$l_{coM_{leg}} = \frac{\left(m_{snk}.l_{coM_{snk}}\right) + \left(m_{\text{foot}}.\left(l_{\text{snk}} + l_{coM_{foot}}\right)\right)}{m_{leg}} \quad (9)$$

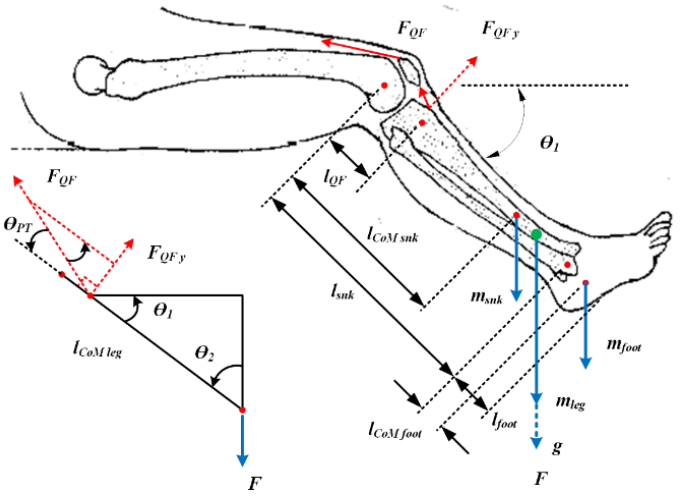


**Fig. 3.** Parameters required for calculating the quadriceps force (FQF)

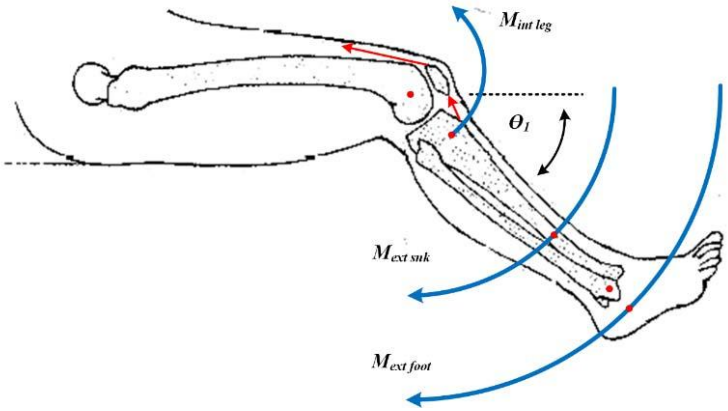


**Fig. 4.** Internal torque of the lower leg ($M_{int_{leg}}$)

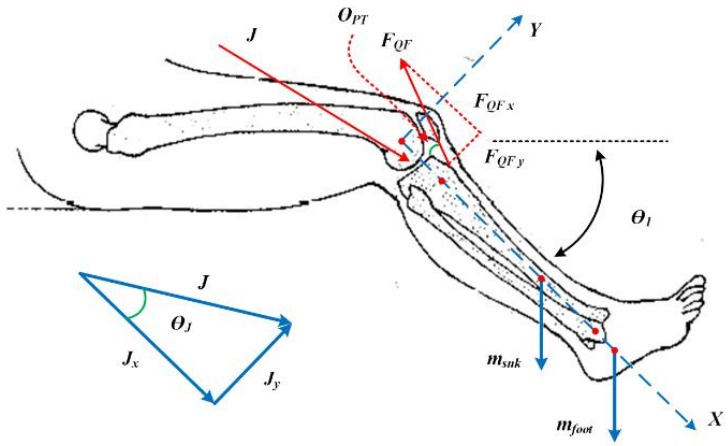


**Fig. 5.** Calculation of the reaction force ($J_F$) in the knee joint.

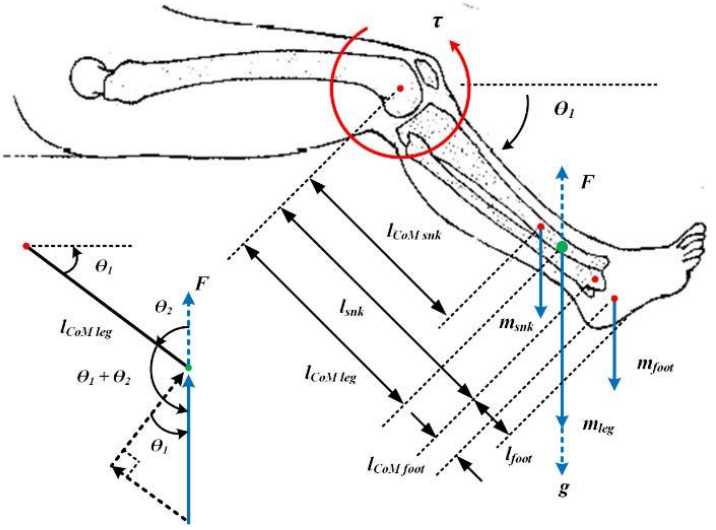


**Fig. 6.** Modeling of the knee joint for calculating the generated torque in the knee joint.

The mass of the leg and the length of the center of mass of the leg are denoted by $m_{leg}$ and $l_{coM_{leg}}$, respectively. The final equation for calculating the torque in the knee joint is presented in equation (10). In this equation, $\tau_{knee}$ represents the required torque to hold the leg, and $F_{coM_{leg}}$ is the force applied at the center of mass of the leg at angle $\theta_1$.

$$\tau_{knee} = F_{coM_{leg}}.l_{coM_{leg}}.\mathrm{Cos}\,\theta_1 = m_{leg}.g.l_{coM_{leg}}.\mathrm{Cos}\,\theta_1 = 9.8\,.\left(m_{snk}.l_{coM_{snk}}\right) + \left(m_{\mathrm{foot}}\,.\left(l_{\mathrm{snk}} + l_{coM_{foot}}\right)\right).\mathrm{Cos}\,\theta_1 \quad (10)$$

## 4. 3D CONCEPTUAL DESIGN OF THE KNEE REHABILITATION ROBOT SYSTEM

Figure 8 shows the 3D conceptual design of the knee rehabilitation robot system. The goal of this design is to develop a robotic arm with one degree of freedom (1-DoF) for controlled, repetitive exercises aimed at improving the range of motion of the knee joint. The prototype system consists of a seating platform where the human torso rests, while the robotic arm moves the distal part of the lower limb to ensure the knee joint's range of motion. Since the design focuses solely on the movement of one leg (the right leg), the robotic arm and its associated mechanical setup are fixed on the right side of the seating platform. For the design and testing of the system, knee flexion up to 90 degrees (the vertical position of the distal part of the leg in a seated state) is considered as the starting point (0 degrees) for range of motion exercises, extending up to 25 degrees of extension. The mechanical components of the system include: a DC motor model SPG S8D40-24A S8KA10B1, a high-precision potentiometer (model M249), pulleys, pulley belts, primary shaft, secondary shaft, a torque sensor (model KMS-40), a rotary encoder, a mechanical arm, and a lower leg holder.

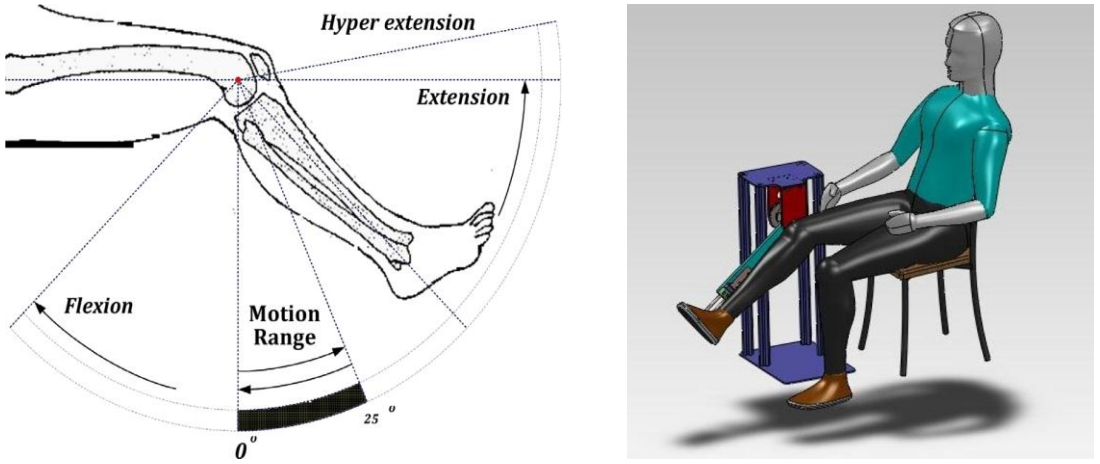


**Fig. 7.** 3D conceptual design of the proposed prototype for rehabilitation.

## 5. DYNAMIC MODELING OF THE SYSTEM ACTUATOR

The dynamic model of the knee joint can be combined with a mass-spring-damper system, as shown in Figure 8. The impedance parameters of the human knee joint are considered as the inertia matrix ($I_K$), the Coriolis and centrifugal force vector ($C$), the damping coefficient matrix ($B$), the knee stiffness matrix ($K$), and the gravitational vector applied to the lower leg piece ($G$). The natural dynamics of the lower leg piece are presented in equation (11), which can be simplified by considering $(B + C) = B_K$ and $(K + G) = K_K$, as shown in equation (12).

$$\tau_k = I_k\ddot{\theta} + (C + B)\dot{\theta} + (K + G)\theta \tag{11}$$

$$B_k\dot{\theta} + K_K\theta = \tau_k - I_k\ddot{\theta} \tag{12}$$

In this equation, $\theta$ and $\tau_K$ represent the knee joint angle and the torque vector, respectively, with $I_K$ considered as a constant. The matrix form of equation (12) for different states ($s_1$, $s_2$, ..., $s_n$) can be modeled as shown in equation (13), where $\theta_{s1}, \theta_{s2}, \dots, \theta_{sn}$ and $b_{s1}, b_{s2}, \dots, b_{sn}$ are the angular displacements and residual forms in different states.

$$\begin{bmatrix} \dot{\theta}_{S1} & \theta_{S1} \\ \dot{\theta}_{S2} & \theta_{S2} \\ \vdots & \vdots \\ \dot{\theta}_{Sn} & \theta_{Sn} \end{bmatrix} \begin{bmatrix} B_K^* \\ K_K^* \end{bmatrix} = \begin{bmatrix} b_{S1} \\ b_{S1} \\ \vdots \\ b_{S1} \end{bmatrix}, Here \begin{cases} b_{S1} = \tau_{k_{S1}} - I_{k_{S1}}\ddot{\theta}_{S1} \\ b_{S2} = \tau_{k_{S2}} - I_{k_{S2}}\ddot{\theta}_{S2} \\ \vdots \\ b_{Sn} = \tau_{k_{Sn}} - I_{k_{Sn}}\ddot{\theta}_{Sn} \end{cases} \tag{13}$$

Equation (13) can be generally expressed as $AX^* = b$, where the angular state vector, impedance vector, and residual vector are represented by $A$, $X^*$, and $b$, respectively. Now, the Least Squares Estimation (LSE) method, as shown in equation (14), can be used to estimate the impedance parameters. The necessary formulation for estimating the impedance parameters for two states (state 1 and state 2) is provided in equation (15).

$$A^T AX^* = A^T b \tag{14}$$

$$\left.\begin{aligned} B_K^* &= \frac{RV - QU}{PR - Q^2} \\ K_K^* &= \frac{U - Q(RV - QU)}{R(PR - Q^2)} \\ P &= \dot{\theta}_1^2 + \dot{\theta}_2^2 \\ Q &= \theta_1\dot{\theta}_1 + \theta_2\dot{\theta}_2 \\ R &= \theta_1^2 + \theta_2^2 \\ U &= \tau_1\theta_1 + \tau_2\theta_2 - I_k(\theta_1\ddot{\theta}_1 + \theta_2\ddot{\theta}_2) \\ V &= \tau_1\dot{\theta}_1 + \tau_2\dot{\theta}_2 - I_k(\dot{\theta}_1\ddot{\theta}_1 + \dot{\theta}_2\ddot{\theta}_2) \end{aligned}\right\} \quad (15)$$

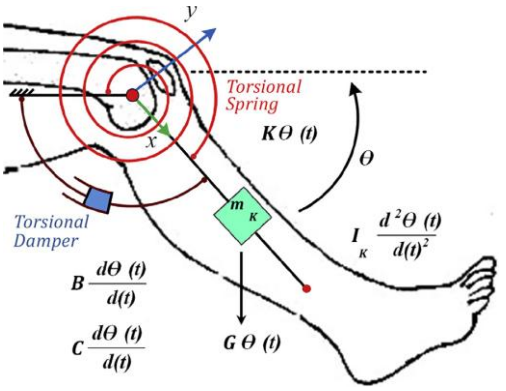


**Fig. 8.** Conceptual dynamic model of the torsional mass-spring-damper knee joint model

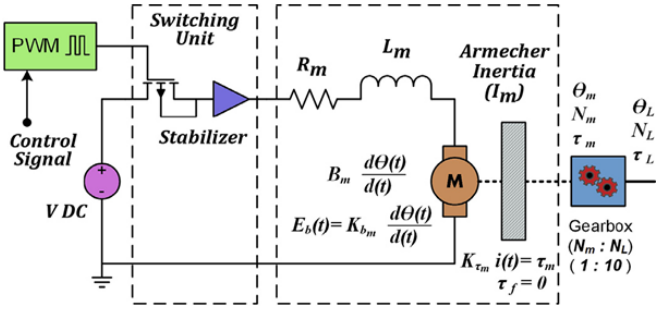


**Fig. 9.** Electromechanical actuator system diagram

For modeling the dynamic behavior of the actuator system, the electromechanical actuator conceptual diagram is shown in Figure 9. The applied voltage ($v(t)$) generates the current ($i(t)$) (denoted by γ(t) in equation (16) due to typographical issues) that passes through the motor coil and produces the rotor torque ($\tau_m$), which is proportional to its magnitude. $I_m$ is the effective inertia of the armature. The back electromotive force (EMF) ($E_b(t)$) is produced due to the angular deviation ($\theta(t)$) of the armature. EMF is proportional to the angular speed ($\theta'(t)$) of the rotor. The input-output ratio of the actuator gearbox is $Nm : NL = 1 : 10$, with frictional force neglected. Based on these electromechanical model characteristics, two fundamental equations for the electrical circuit dynamics and mechanical dynamics, as shown in equation (16), can be determined, where the frictional torque ($\tau_{fm}$) is neglected.

$$\left.\begin{aligned} L_m\dot{\gamma}(t) + K_{b_m}\dot{\theta}_m(t) + R_m\gamma(t) &= v_m(t) \\ I_m\ddot{\theta}_m(t) + B_m\dot{\theta}_m(t) + \frac{N_m}{N_l}(\tau_l) &= K_{\tau_m}\gamma(t) \end{aligned}\right\} \quad (16)$$

Here, $R_m$ ،$L_m$ ،$K_{bm}$ ،and $K_{\tau m}$ represent the electrical components such as resistance, inductance, back electromotive force (EMF), and the torque constant of the actuator. The mechanical constants of the equation include the armature inertia ($I_m$), viscous friction ($B_m$), and the external load ($\tau_L$).

## 6. RESULTS

This section presents the results for athletes of different heights and weights. Based on the mathematical modeling of the human foot and knee joint, simulations were performed using MatLab to observe the force and torque behavior at various angles of knee joint extension. The seated position was considered for this study. The results are shown in Table 2.

**Table 2.** Force and Torque values at 25 degrees knee joint angle for different weights and heights

| | | Weight (kg) | | | | | | | | |
|---|---|---|---|---|---|---|---|---|---|---|
| Heights | | ۶۰ | ۶۵ | ۷۰ | ۷۵ | ۸۰ | ۸۵ | ۹۰ | ۹۵ | ۱۰۰ |
| ۱.۶۵ | R | ۳۶.۱۲ | ۳۹.۴ | ۴۲.۶۸ | ۴۵.۹۶ | ۴۹.۲۴ | ۵۲.۵۲ | ۵۵.۸ | ۵۹.۰۸ | ۶۲.۳۶ |
| | M | ۰.۷۵۷۳۷ | ۰.۸۳۰۷۵ | ۰.۹۰۴۱۳ | ۰.۹۷۷۵۱ | ۱.۰۵۰۸۹ | ۱.۱۲۴۲۷ | ۱.۱۹۷۶۵ | ۱.۲۷۱۰۳ | ۱.۳۴۴۴۱ |
| | τ | ۷.۶۱۲ | ۸.۳۲۱ | ۹.۰۲۳ | ۹.۷۳۸ | ۱۰.۴۴۷ | ۱۱.۴۵۶ | ۱۱.۸۶۲ | ۱۲.۵۷۳ | ۱۳.۲۸۲ |
| ۱.۷ | R | ۳۵.۰۳ | ۳۸.۲۱ | ۴۱.۳۹ | ۴۴.۵۷ | ۴۷.۷۵ | ۵۰.۹۳ | ۵۴.۱۱ | ۵۷.۲۹ | ۶۰.۴۷ |
| | M | ۰.۷۸۱ | ۰.۸۵۶۷ | ۰.۹۲۲۴ | ۱.۰۰۸۱ | ۱.۰۸۳۸ | ۱.۱۵۹۴ | ۱.۲۳۵۱ | ۱.۳۱۰۸ | ۱.۳۸۶۴ |
| | τ | ۷.۸۴۹۹ | ۸.۵۸۱ | ۹.۳۱۱۵ | ۱۰.۰۴۲۴ | ۱۰.۷۷۳۲ | ۱۱.۵۰۴۱ | ۱۲.۲۳۴۹ | ۱۲.۹۶۵۸ | ۱۳.۹۶۶۶ |
| ۱.۷۵ | R | ۳۳.۹۶ | ۳۷.۰۵ | ۴۰.۱۳ | ۴۳.۲۱ | ۴۶.۳۱ | ۴۹.۳۸ | ۵۲.۴۷ | ۵۵.۵۵ | ۵۸.۳۴ |
| | M | ۰.۸۰۵۴ | ۰.۸۸۳۴ | ۰.۹۶۱۵ | ۱.۰۳۹۵ | ۱.۱۱۷۶ | ۱.۱۶۵۶ | ۱.۲۷۳۶ | ۱.۳۵۱۵ | ۱.۴۲۹۷ |
| | τ | ۸.۰۹۵۲ | ۸.۸۴۸۸ | ۹.۶۰۲۵ | ۱۰.۳۵۶۲ | ۱۱.۱۰۹۹ | ۱۱.۸۶۳۶ | ۱۲.۶۱۷۳ | ۱۳.۳۷۱۰ | ۱۴.۱۲۴۷ |
| ۱/۸ | R | ۳۲.۹۴ | ۳۵.۹۳ | ۳۸.۹۲ | ۴۱.۹۱ | ۴۴.۹ | ۴۷.۸۹ | ۵۰.۸۸ | ۵۳.۸۷ | ۵۶.۸۶ |
| | M | ۰.۸۳۰۶ | ۰.۹۱۱۰ | ۰.۹۹۱۵ | ۱.۰۷۲۰ | ۱.۱۵۲۵ | ۱.۲۳۳۰ | ۱.۳۱۳۴ | ۱.۳۹۳۹ | ۱.۴۷۴۴ |
| | τ | ۸.۳۴۸۲ | ۹.۱۲۵۴ | ۹.۹۰۲۶ | ۱۰.۶۷۹۹ | ۱۱.۴۵۷۱ | ۱۲.۲۳۴۴ | ۱۳.۰۱۱۶ | ۱۳.۷۸۸ | ۱۴.۵۶۶۱ |
| ۱.۸۵ | R | ۳۱.۹۴ | ۳۴.۸۴ | ۳۷.۷۴ | ۴۰.۶۳ | ۴۳.۵۲ | ۴۶.۴۴ | ۴۹.۳۲ | ۵۲.۲۴ | ۵۵.۱۵ |
| | M | ۰.۸۵۶۷ | ۰.۹۳۹۷ | ۱.۰۲۲۷ | ۱.۱۰۵۷ | ۱.۱۸۸۷ | ۱.۲۷۱۸ | ۱.۳۵۴۸ | ۱.۴۳۷۸ | ۱.۵۲۰۸ |
| | τ | ۸.۶۰۹۱ | ۹.۴۱۰۶ | ۱۰.۲۱۲۱ | ۱۱.۰۱۳۷ | ۱۱.۸۱۵۲ | ۱۲.۶۱۶۷ | ۱۳.۴۱۸۳ | ۱۴.۲۱۹۸ | ۱۵.۰۲۱۳ |
| ۱.۹ | R | ۳۰.۹۷ | ۳۳.۷۸ | ۳۶.۶ | ۳۹.۴۱ | ۴۲.۲۲ | ۴۵.۰۳ | ۴۷.۸۵ | ۵۰.۶۵ | ۵۳.۴۷ |
| | M | ۰.۸۸۳۵ | ۰.۹۶۹۱ | ۱.۰۵۴۷ | ۱.۱۴۰۳ | ۱.۲۲۵۹ | ۱.۳۱۱۵ | ۱.۳۹۷۱ | ۱.۴۸۲۷ | ۱.۵۶۸۳ |
| | τ | ۸.۸۷۸۱ | ۹.۷۰۴۷ | ۱۰.۵۳۱۳ | ۱۱.۳۵۷۹ | ۱۲.۱۸۴۵ | ۱۳.۰۱۱۱ | ۱۳.۸۳۷ | ۱۴.۶۶۴۲ | ۱۵.۴۹۰۸ |

## 7. CONCLUSION

This paper presents the development of a robotic rehabilitation system for knee joint range of motion exercises. The system is an experimental prototype with one degree of freedom (1-DoF), designed exclusively for right knee range of motion exercises. In this study, a seated position was considered, where the torso and thigh are at rest. The control mechanism was designed and simulated through state-space modeling, and the parallel control architecture of three compensators reflects the impedance estimation of the knee joint and torque feedback. The proposed mechanism considers human leg inertia as an independent input, determined based on the body's index parameters, and is used in the knee joint impedance estimation. The system responses ensure that the prototype can be used for practical experiments with human patients. Although the prototype has some limitations, such as restricting the range of motion to 25 degrees and being designed only for right knee exercises, the system demonstrates its potential for practical trials. Further modifications and improvements to the system could support its practical application and allow it to be used as a portable therapeutic device for home use.

**Declaration**

We acknowledge that we used ChatGPT to enhance the academic writing of our manuscript while ensuring the originality and integrity of our work.

**Transparency Statement**

The data supporting this study are available upon reasonable request to the corresponding author, subject to ethical and confidentiality considerations.

**Acknowledgments**

We would like to express our gratitude to all individuals who contributed to this project.

**Declaration of Interest**

The authors declare that they have no competing interests.

**Funding**

This research received no specific grant from any funding agency, commercial, or not-for-profit sectors.

**REFERENCES**

[1] Sawhney, R., et al. (1990). Quadriceps exercise following anterior cruciate ligament reconstruction without anterior tibial displacement. In American Conference of the American Physical Therapy Association. Anaheim, CA.

[2] Beynnon, B. D., et al. (1995). Anterior cruciate ligament strain behavior during rehabilitation exercises in vivo. The American Journal of Sports Medicine, 23(1), 24-34. https://doi.org/10.1177/036354659502300105

[3] Paulos, L., et al. (1981). Knee rehabilitation after anterior cruciate ligament reconstruction and repair. The American Journal of Sports Medicine, 9(3), 140-149. https://doi.org/10.1177/036354658100900303

[4] Renström, P., et al. (1986). Strain within the anterior cruciate ligament during hamstring and quadriceps activity. The American Journal of Sports Medicine, 14(1), 83-87. https://doi.org/10.1177/036354658601400114

[5] Arms, S. W., et al. (1984). The biomechanics of anterior cruciate ligament rehabilitation and reconstruction. The American Journal of Sports Medicine, 12(1), 8-18. https://doi.org/10.1177/036354658401200102

[6] Sachs, R. A., et al. (1989). Patellofemoral problems after anterior cruciate ligament reconstruction. The American Journal of Sports Medicine, 17(6), 760-765. https://doi.org/10.1177/036354658901700606

[7] Shelbourne, K. D., & Nitz, P. (1992). Accelerated rehabilitation after anterior cruciate ligament reconstruction. Journal of Orthopaedic & Sports Physical Therapy, 15(6), 256-264. https://doi.org/10.2519/jospt.1992.15.6.256

[8] Akhtaruzzaman, M., Shafie, A. A., & Khan, M. R. (2016). A review on lower appendicular musculoskeletal system of human body. IIUM Engineering Journal, 17(1), 83-102. https://doi.org/10.31436/iiumej.v17i1.571

[9] Dempster, W. T. (1955). Space requirements of the seated operator. WADC-55-159. Wright-Patterson Air Force Base, OH.

[10] Leva, P. (1996). Adjustments to Zatsiorsky-Selunayov's segment inertia parameters. Journal of Biomechanics, 29, 1223-1230. https://doi.org/10.1016/0021-9290(95)00178-6

[11] Tozeren, A. (2000). Human body dynamics: Classical mechanics and human movement. Springer-Verlag.

[12] Laschowski, B. (2016). Biomechanical modeling of Paralympic wheelchair curling (Master's thesis, University of Waterloo).

[13] Santschi, W. R., Dubois, J., & Omoto, C. (1963). Moments of inertia and centers of gravity of the living human body. AD-410-451. Wright-Patterson Air Force Base, OH. https://doi.org/10.21236/AD0410451

[14] Krishnan, R. H., Devanandh, V., Brahma, A. K., & Pugazhenthi, S. (2016). Estimation of mass moment of inertia of human body, when bending forward, for the design of a self-transfer robotic facility. Journal of Engineering Science and Technology, 11(2), 166-176.

[15] Oatis, K. A. (2009). Kinesiology: The mechanics and pathomechanics of human movement (2nd ed., Chapter 43, pp. 791-805). Lippincott Williams & Wilkins, a Wolters Kluwer business.